Design Optimization of Coanda Effect Based UAV using CFD Simulations

By

SAAD ALI LIAQAT

FALL2015-RIME00000147533

Supervisor

Dr. YASAR AYAZ

Department Of Robotics and Intelligent Machine Engineering

School of Mechanical and Manufacturing Engineering (SMME)

National University of Sciences and Technology (NUST)

Islamabad

August, 2019

Design Optimization of Coanda Effect Based UAV using CFD Simulations

SAAD ALI LIAQAT
FALL2015-RIME00000147533

A thesis submitted in partial fulfillment of the requirements for the degree of *Master of Science* in Robotics and Intelligent Machine Engineering

Thesis Supervisor:
Dr. YASAR AYAZ

Thesis Supervisor's Signature: _____

DEPARTMENT OF ROBOTICS AND INTELLIGENT MACHINE ENGINEERING
SCHOOL OF MECHANICAL & MANUFACTURING ENGINEERING
NATIONAL UNIVERSITY OF SCIENCES AND TECHNOLOGY, ISLAMABAD
AUGUST, 2019

DECLARATION

I certify that this research work titled "*Design Optimization of Coanda Effect Based UAV using CFD Simulations"* is my own work. The work has not been presented elsewhere for assessment. The material that has been used from other sources it has been properly acknowledged / referred.

SAAD ALI LIAQAT

FALL2015-RIME00000147533

THESIS ACCEPTANCE CERTIFICATE

Certified that final copy of MS thesis written by Mr. Saad Ali Liaqat (Reg No. Fall2015-RIME00000147533) of SMME has been vetted by undersigned, found completed in all respects as per NUST Statues / Regulations, is free of plagiarism, errors, and mistakes and is accepted as partial fulfillment for award of MS/MPhil Degree. It is further certified that necessary amendments as pointed out by GCE members of the scholar have also been incorporated in the said thesis.

Signature: _____

Name of Supervisor: _____

Date: _____

Signature of (HoD): _____

Date: _____

Signature of (Principal): _____

Date: _____

PLAGIARISM CERTIFICATE (TURNITIN REPORT)

This thesis has been checked for Plagiarism. Turnitin report endorsed by Supervisor is attached.

Signature of Student
SAAD ALI LIAQAT
FALL2015-RIME00000147533

Signature of Supervisor

COPYRIGHT STATEMENT

ACKNOWLEDGEMENTS

First of all praise and thanks to Almighty Allah who has showered countless blessings upon me during my MS study in SMME NUST and during my whole life.

I would like to express my utmost gratitude to my supervisor Dr. Yasar Ayaz for his mentoring, guidance, motivation and for inculcating in me a quest of knowledge. Throughout the thesis I find him helping and encouraging my novel ideas.

In addition to this I would also like to thank Dr. Jawad Khan, Dr. Muhammad Sajid and Dr. Ali Zaidi for helping, supporting and rectifying my research methodology and ideas.

Finally, I would like to extend my love to my family who have always supported me in my endeavours and encouraged me to achieve my goals through hard work and perseverance. Moreover, I would like to thank all my friends for their support and assistance.

I dedicate this thesis to my parents

ABSTRACT

Recently, Unmanned Aerial Vehicles (UAVs) have gained immense importance in many fields including agriculture, robotics, surveillance, mapping, search and rescue due to their ability to cover long distances quickly and hover above the surface. This research presents design optimization of a relatively new type of UAV which utilizes Coanda effect for lift augmentation. Computational fluid dynamics analysis is carried out to understand lift mechanism due to Coanda Effect for two common configurations as baseline models to gain insight into the lift generation. Propeller based configuration in which propeller is above the Coanda surface is found to be unfavorable for lift augmentation while centrifugal fan configuration is found to be viable. Analysis highlighted two important factors which necessitates design changes to improve performance. Variations in curved Coanda surface and lower part is carried out which improved the net lift generated. Finally the improved shape is optimized using adjoint solver. This novel and optimized model is called RISE Coanda which lowers the pressure drag and increase the net lift by approximately 50% as compared to baseline models.

Key Words: *Adjoint, Coanda effect, CFD, lift augmentation, optimization, UAV, VTOL*

TABLE OF CONTENTS

LIST OF FIGURES

LIST OF TABLES

CHAPTER 1: INTRODUCTION

1.1 Background

An unmanned or uninhabited aerial vehicle (UAV), commonly known as a drone is a type of an aircraft which does not have any human pilot aboard. Usually they are controlled piloted remotely by the pilots on ground in ground control stations or they may be controlled autonomously by onboard computers, sensors and other means of navigation. Depending upon their design and configuration, unmanned aerial vehicles are divided into two main classes:

- Fixed-wing UAV
- Rotary-wing UAV

A fixed-wing UAV is an aircraft as shown in fig 1.1, which is capable of flying using wings that generate lift caused by the vehicle's forward airspeed and the shape of its wing. Net lift is produced due to the pressure differential between upper and lower surface of the wing.

Figure 1.1 MQ-9 Reaper fixed wing UAV

A rotary-wing UAV is an aircraft as shown in fig 1.2 and 1.3, which is capable of flight using propellers to produce thrust to overcome weight by the application of both Bernoulli's principle and Newton's third law. Their VTOL (Vertical Takeoff and Landing) capability makes them ideal for many indoor and outdoor applications.

Figure 1.2 MQ-8 Fire Scout

Figure 1.3 DJI Phantom Drone

In rotary wing UAVs, quad copter (having four propellers for thrust and directional controls) have gained immense importance due to their stable hovering abilities in both

indoor and outdoor environment. Unmanned Aerial Vehicles (UAVs) of different types have gained immense popularity and acceptability in civil as well as military applications. They are being used in aerial photography and mapping, remote sensing, disaster search and rescue, traffic monitoring, novel agricultural techniques, inspection of building or other infrastructure, providing wireless connectivity as a substitute to long distance cabling and added cost and much more due to their ease of operation, maneuverability and hovering ability[1]. However, one of the main drawback of rotary wing UAV is the low endurance as the lifting force comes mainly from the thrust produced by the propellers. There are many other configurations developed and tested to increase the endurance of rotary UAVs which include tricopter, tilt rotor and hybrid configurations. Recently, a new type of UAV is being researched known as Coanda UAV which utilizes Coanda Effect to produce lift in addition to the lift produced by the propellers.

Coanda Effect is named after a Romanian aerodynamicist Henri Coanda which explains the attachment of a fluid to a convex surface. When a viscous fluid is allowed to flow through a jet or orifice, fluid from the surrounding is entrained due to the viscous forces acting on the molecules and this creates a low pressure area around the flow stream. If a convex surface is brought near the flow, fluid will attach to the surface due to a low pressure area [2], [3]. Henri Coanda implemented this effect in his patent but due to insufficient technological support he was not successful. Later after almost 50 years GFS projects, a company based in UK designed, developed and tested a prototype VTOL UAV which utilizes Coanda effect to augment the lift production. It employed single rotor and control fins to counter the torque. After its successful flight many other researchers have shifted their focus on a relatively less researched area of utilizing Coanda effect to augment the

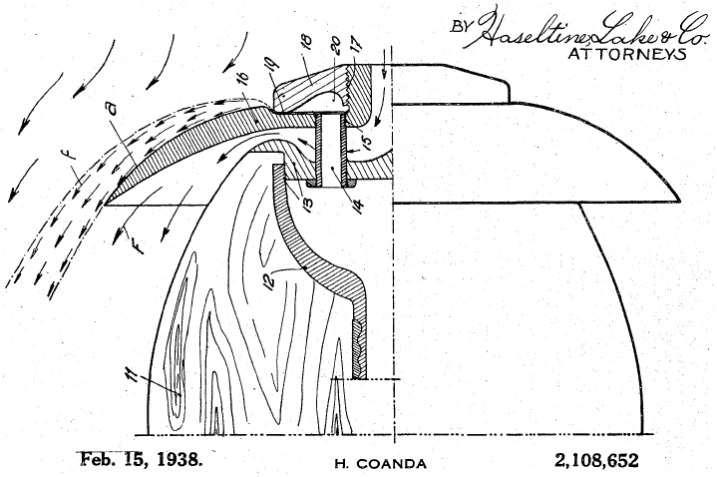

Figure 1.4 Henri Coanda patent (1936)

lift. There are many benefits of this design which include safety as rotors are enclosed, VTOL ability and payload not coming into the airflow. Still there is a huge gap for research. This study aims to introduce novel design to optimize the design of Coanda UAV to gain greater endurance and range. In addition to this, Coanda effect has applications in aircraft flaps, NOTAR (No Tail Rotor) helicopters and lift augmentation using jet engine exhaust over the wings.

In this study we investigate the two baseline configurations of Coanda UAV which are propeller with the Coanda surface and centrifugal fan with the Coanda surface. Many authors have carried out CFD analysis of Propeller Coanda combination and in each experiment lift comes out to be negative. Although these Coanda UAVs fly but their lift is primarily from the rotor thrust. Lift augmentation provided by the Coanda surface is less as compared to high pressure from the propeller pushing the vehicle in the opposite direction. Furthermore, no study can be found which addresses the low pressure area underneath the UAV known as wake. This study introduces a new Coanda UAV which has been optimized to increase lift from curved surface as well as eliminating the low pressure wake by mixing it with high velocity flow to reduce drag which resulted in an increase in the total lift.

1.2 Problem Definition

One of the most important performance parameter of an aircraft or Unmanned Aerial Vehicle (UAV) is range and endurance. Range can defined as the distance an aircraft can fly between takeoff and landing with on board fuel while the endurance can be defined as the amount of time an aircraft can remain airborne with on board fuel. Both these parameters are limited by the design of an aircraft. For optimization, there is need to have a good balance of trade off between performance, stability, control and safety.

1.3 Motivation

Design of an optimized Coanda Effect based UAV which increases range and endurance through lift augmentation. Furthermore, this type of UAV can be a potential candidate for the research and development in aerial robotics.

CHAPTER 2: RELATED WORK

In this section the important work done by the researchers in the design and development of Coanda Effect based UAV will be explained. A UK based company AESIR formerly GFS projects limited designed and developed a UAV based on the Coanda Effect [4]. It consists of a semi spherical hull with an enclosed propeller on top. Its main purpose is to develop a stable and novel form of UAV which can traverse through and around the obstacles without damaging the propeller as shown in fig 2.1. It has the versatility to range in size from few centimeters to meters. As there was only one motor / propeller for propulsion so there was a need to cancel out the torque produced by the motor. This design employed fins (which are adjustable through servo motor to change angle of attack and hence the force) attached to the body to counteract the torque and also act as a control surface for yawing motion. In addition to this servo controlled flaps are used to control rolling and pitching moment.

Figure 2.1 GFS-UAV

Another study based on the GFS UAV design in which preliminary design of a Coanda test bed known as Coanda JLT Craft as shown in fig 2.2 was carried out by Ping et al.[5]. The experiment consists of a Coanda curved surface which was placed in a flow coming from the wind tunnel. Coanda surface is attached to the weighing machine to calculate the lift produced. Wind tunnel

was operated at different velocities and optimum velocity was found. As the velocity increases, lift increases until there comes a point from where it begins to decrease due to the flow separation. Lift coefficient which is an important parameter in aerodynamics is calculated at different velocities. Moreover, instead of fins, coaxial rotors as found on helicopters were used to control yawing moment and prototyping was done. Similarly in another experiment Ping et al [6].

Figure 2.2 Coanda JLT Craft

Utilizing the same test bed to find the relationship between angle of attack of Coanda surface and the lift generated. A JLT reference line is used to mark the zero angle of attack. It applied the same principle on the Coanda effect as applied on airfoils on a conventional aircraft. It shows the variation of lift coefficient with changing angle of attack. Similarly, he shows how to steer a Coanda UAV using a body surfaces at different angle of attack. Other design parameters were also explored. In order to find the optimum ratio of width to height of a Coanda spherical body different design J. Jeon et al [7] designed and experimentally validated the Coanda Effect saucer. It also uses anti torque fins. Airfoil circulation concept was used for experimentation in which an airfoil is rotated 360 and the conditions were simulated as an airfoil would experience. This study found out that most efficient configuration was when air is blowing over the top surface and inducing air from below through center hole [8]. Many studies were aimed at improving the Coanda surface / profile to increase the lift using CFD (Computational Fluid Dynamics) simulations [9], [10]. Out of all the designs oval shape was chosen because it is simple to design. An optimum ratio of height

over width is found to be 0.875. Coanda surface is divided into three sections. Section one is below the propeller to change the flow direction while section two is responsible for the lift generation and the third section is used to control the flow separation. CFD simulations were performed iteratively by varying the dimensions of second and third section and calculating the resultant lift. In addition to this dynamic modelling was done to verify the controllability of Coanda effect UAV. In all these configurations where propeller is used as a propulsion device, there is a net negative lift generated due to the high pressure air from the propeller hitting the Coanda surface before changing the direction.

H. Djojodihardjo [11] apply fundamental principle utilizing mass and momentum conservation laws to analyze the generation of lift on Coanda Effect UAV and developed a mathematical model. There are two types of flow configurations cylindrical and spherical. The analysis highlights the three sources of lift generation which include lift due to Coanda jet momentum, the lift due to pressure differential between upper and lower surface and the lift due to the thrust from propeller. Coanda effect is being utilized in other domains also. An airfoil is fitted with a Coanda jet to delay the flow separation and adding energy to the boundary layer to stay attached to the airfoil. Similarly, wind turbines blades are fitted with Coanda jets for lift augmentation. A computational study performed to analyze the aerodynamic performance of wind turbine with Coanda jet confirms the lift augmentation [12]. In another study some performance measures were established to evaluate the performance of Coanda Effect based UAV and compare it with the CFD simulations results. Flight dynamics analysis was also carried for hovering and translational movement phase of flight to determine the effects of actuator in each phase [13].

Some other researchers used geometry parameterization techniques to explore the multi-dimensional design space to find the optimum shape of Coanda surface to produce maximum lift. Bernstein polynomial is used to optimize the shape and maneuverability by thrust vectoring (changing the attitude by changing the direction of thrust) [14]. C. Gan et al [15], introduced logarithmic spiral surface for Coanda surface to evaluate the lift generation. It describes how the Coanda jet thickness increases and the velocity decreases along the surface. It also emphasizes a wider jet will produce greater lift as compared to thinner jets.

Implementation of classical and modern control theory is essential in almost every application requiring regulation of a system output. In order to implement any control law, there must be a mathematical model of a physical system or a transfer function of a system. In this

regard, J. Y. Lee [16] developed a dynamic model of Coanda UAV and the corresponding motor mapping was used in simulations and later implemented on a Pixhawk autopilot controller to check the dynamic response of a system. To gain insight into the dynamic response of a system, either you have to develop a mathematical model or experimentally determine the response by measuring inputs and outputs of a system. The latter is known as system identification in control theory. Mathematical model do not cater for the non linearities and coupling of various parameters. A study by Banazadeh et al [17], using system identification technique in frequency domain suggested that a closed loop feedback system is necessary for the intrinsically unstable Coanda UAV.

In Computational Fluid Dynamics (CFD), optimization algorithms are used frequently to optimize the given shape for various applications. It includes structural, electromagnetic, aerodynamics, thermodynamics etc. Out of many different optimization algorithms, adjoint optimization is preferred due to its low computational cost [18].

CHAPTER 3: ANALYSIS

This section will explain in detail the analytical as well as the computational analysis of the Coanda UAV.

3.1 Analytical Analysis

With reference to the fig (1), which shows the schematics of Coanda UAV control volume. In this figure 'R' represents radius of the Coanda surface, 'v' is the velocity of the Coanda jet, 'h' is the thickness of Coanda jet and 'Pa' is the ambient atmospheric pressure. The lift because of Coanda effect is generated by the blanket formed by the airflow over the curved surface as derived by [11].

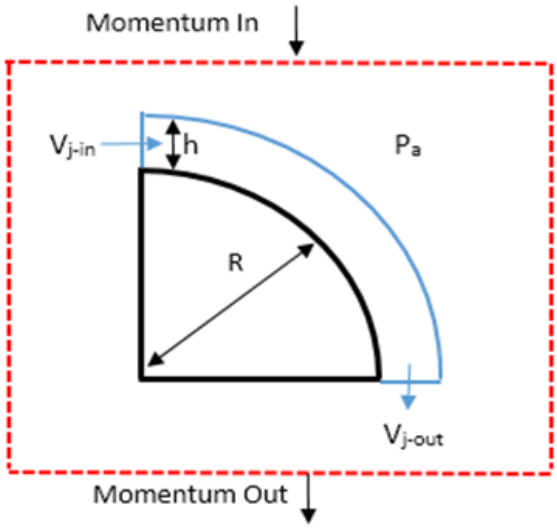

Figure 3.1 Coanda UAV control volume schematics

For analysis, laws of conservation of mass, energy and momentum, which form the fundamental axioms of fluid dynamics were utilized. For conservation of mass, continuity equation is applied to the control volume fig 2. Given by the equation as used by [13]

$$\rho_{in} V_{j-in} A_{in} = \rho_{out} V_{j-out} A_{out} \tag{3.1}$$

Putting the values in the equation (1) for the spherical Coanda UAV, we have

$$\rho . V_{j-in} . 2\pi R_i h_i = \rho . V_{j-out} . 2\pi R_o h_o \quad (3.2)$$

Applying momentum equation in the z-direction

$$Lift_{Momentum-Coanda\ jet\ blanket} = \dot{m}_{out} V_{j-out}$$

$$= 2\pi R_o h_o \rho V^2 \quad (3.3)$$

As there is no contribution of lift so the radial component of momentum balance lift because of Coanda blanket is given by eq (3.3). In addition to this, pressure differential is also responsible for the lift generation due to pressure balance between curved surface of the Coanda UAV wall and the pressure underneath the body. This pressure differential is calculated by applying Bernoulli equation along the stream line in the Coanda blanket. This is given by

$$p_a = p + \frac{1}{2} \rho V_j^2 \quad (3.4)$$

At any point R along the stream line the pressure becomes

$$p = p_a - \frac{1}{2} \rho V_{j\,at\,(R)}^2 \quad (3.5)$$

The lift between two surfaces becomes

$$F = \int_0^{\pi/2} p_{upper}\, 2\pi R^2 \cos\theta d\theta - p_{lower\,.area_{lowersurface}} \quad (3.6)$$

Thus, the total force due to Coanda blanket is equal to sum of Coanda jet momentum balance and the pressure difference created by Coanda blanket. So the final equation becomes

$$Lift_{\substack{Coanda\ jet \\ +\ induced\ pressure}} = 2\pi R h \rho_j V_{j-out}^2 + \pi R^2 \rho_j V_{j-out}^2 \quad (3.7)$$

Equation (3.7) quantifies the lift augmentation provided by the Coanda effect to the Coanda UAV as compared to the conventional VTOL UAVs lifted by the thrust from the propeller / actuator disk only.

3.2 Numerical Analysis

3.2.1 Baseline Models

For numerical analysis two baseline models were analyzed in which one uses axial fan / propeller known as SCoanda, which was designed and optimized by Hyunyong Lee et al [5] and the other uses centrifugal fan by Gan et al. First model was optimized empirically by changing the dimensions of the curved Coanda surface and calculating the Coanda lift force by using CFD. These optimized dimensions were used to make CAD model for this analysis as shown in the fig 3.2. Similarly, second model which is a parametric analysis of Coanda flow by varying the jet height and using logarithmic spiral surfaces as shown in fig 3.3.

3.2.2 Computational Fluid Dynamics (CFD)

Computational Fluid Dynamics (CFD) is a fundamental part of fluid mechanics which is used to analyze, simulate and solve fluid flow problems using numerical analysis techniques and data structures For performing calculations, supercomputers or high end computers are used to simulate the free-stream fluid flow, and the interaction of the fluids with the surfaces having appropriate boundary conditions. It uses Navier-Stokes equations which describe the viscosity of fluid flow. The governing equations are based on three laws of conservation which are mass, momentum and energy conservation. These equations are computed to calculate three unknown variables velocity and pressure. For incompressible flows Navier Stokes equation becomes

$$\rho \frac{D\vec{v}}{Dt} = -\nabla p + \mu \nabla^2 \vec{v} + \rho g \tag{3.8}$$

Where ρ is the density of the fluid, v is the velocity, p is the pressure, μ is the coefficient of viscosity, ∇ is the divergence and g is the gravitational acceleration. There are different types of discretization methods out of which Finite Volume Method (FVM) was adopted. Finite Volume Method (FVM) is used to discretize the domain into sub domains called control volumes. For this analysis, pressure based solver is used as the flow is incompressible. The choice of turbulence modelling is crucial for accuracy of the solution. Turbulence model is a mathematical model to predict the effects of turbulence. In this research, SST k-ω turbulence model is used which is a two-equation eddy-viscosity model [19].

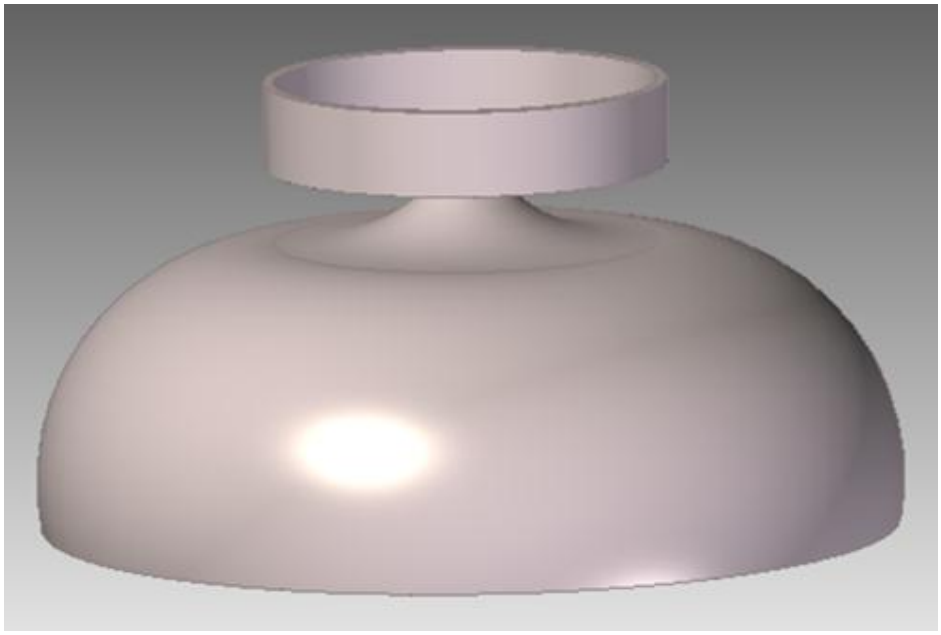

Figure 3.2 Baseline model 1

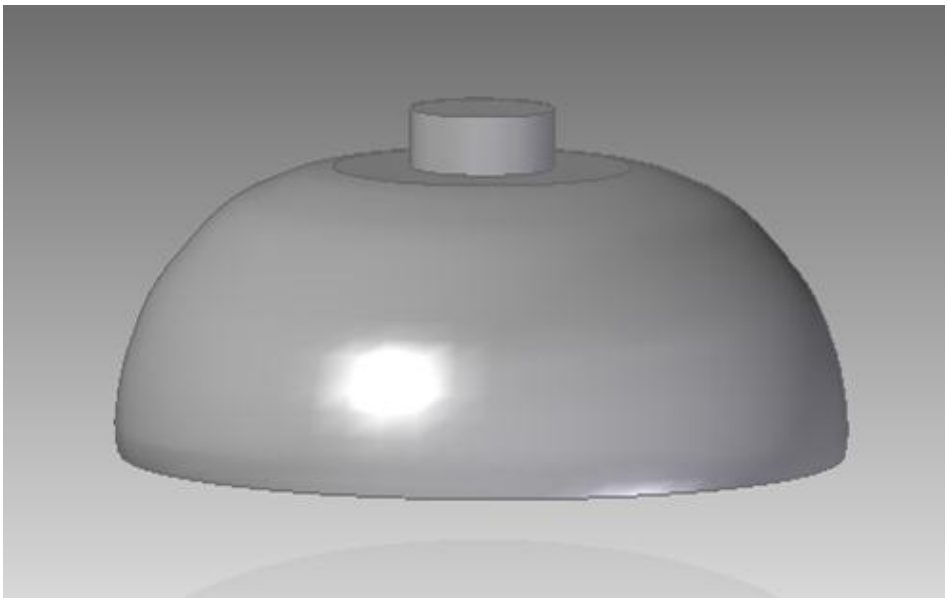

Figure 3.3 Baseline model 2

The shear stress transport (SST) turbulence model serves the dual purpose. Firstly it uses kω formulation for the boundary layer and its inner parts so that the model can be implementable up to the wall through the sub layers. Due to its favorable properties it has gained widespread applications having low Reynolds number. Secondly, the SST model transitions to a k-ε behavior to avoid high sensitivity problem associated with k-ω model to the far upstream turbulence. Many

researchers have used SST k-ω mode because of having good feedback regarding its response in flow separation and adverse pressure gradients. Kinematic eddy viscosity is given by

$$V_T = \frac{a_1 k}{\max(a_1 \omega, SF_2)} \tag{3.9}$$

Turbulence kinetic energy is given by

$$\frac{\partial k}{\partial t} + U_j \frac{\partial k}{\partial x_j} = P_k - \beta^* k\omega + \frac{\partial}{\partial x_j}\left[(v + \sigma_k v_T)\frac{\partial k}{\partial x_j}\right] \tag{3.10}$$

The specific dissipation is the rate of conversion of turbulence kinetic energy into internal energy per unit time and volume given by

$$\frac{\partial \omega}{\partial t} + U_j \frac{\partial \omega}{\partial x_j} - \alpha S^2 - \beta \omega^2 + \frac{\partial}{\partial x_j}\left[(v + \sigma_\omega v_T)\frac{\partial \omega}{\partial x_j}\right] \tag{3.11}$$

3.2.3 Grid Independence

Meshing is one of the most important aspect of CFD which has a huge impact on the results. If the mesh is coarse, it will give poor results and if the mesh is too fine then it will increase computational cost. Therefore, it is critical to carry out grid independence test. This test involves finding the optimum mesh size after which solution is not affected by increasing the mesh size thereby reducing the computational cost. Grid independence test is performed on baseline model at a constant flow velocity of 15 m/s. Three different mesh sizes were used coarse, normal and fine and the Coanda lift was calculated. Fig (3.4) shows the value of lift corresponding to each mesh size. From coarse to medium mesh size, percentage change in lift is 3% while increasing size from medium to fine percentage change is 0.4 %. Thus further mesh refinement is not necessary. In this case orthogonality criteria is also met which states that minimum orthogonality for a mesh should be greater than 0.01. In addition to this maximum skewness is within the acceptable range.

Table 3-1: Grid Independence Study

	Coarse	Medium	Fine
Elements	554230	1027371	2294153
Maximum Skewness	0.82	0.81	0.79
Minimum Orthogonality	0.14	0.16	0.17
Aspect Ratio	4.22	2.35	1.81

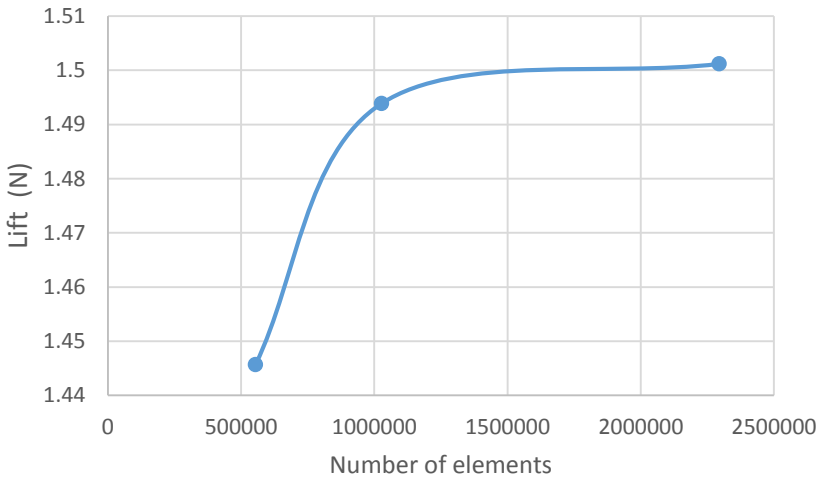

Figure 3.4 Grid independence study

3.2.4 Solution

Computations were carried out with the conditions given above and the convergence criteria was set. Coanda lift was calculated at different velocities which are 5, 10, 15, 20 and 25 m/s for the baseline models. To visualize the flow, pressure contours are plotted for the baseline models as shown in fig (5) and (6). As seen from the fig (5), there is a a Coanda blanket where surface pressure is lower than the surrounding resulting in a lift force. However, there is a high pressure

area just beneath the propeller which pushes the Coanda UAV downward in the direction of drag and weight and this is undesirable. There is another region below the Coanda UAV which can be

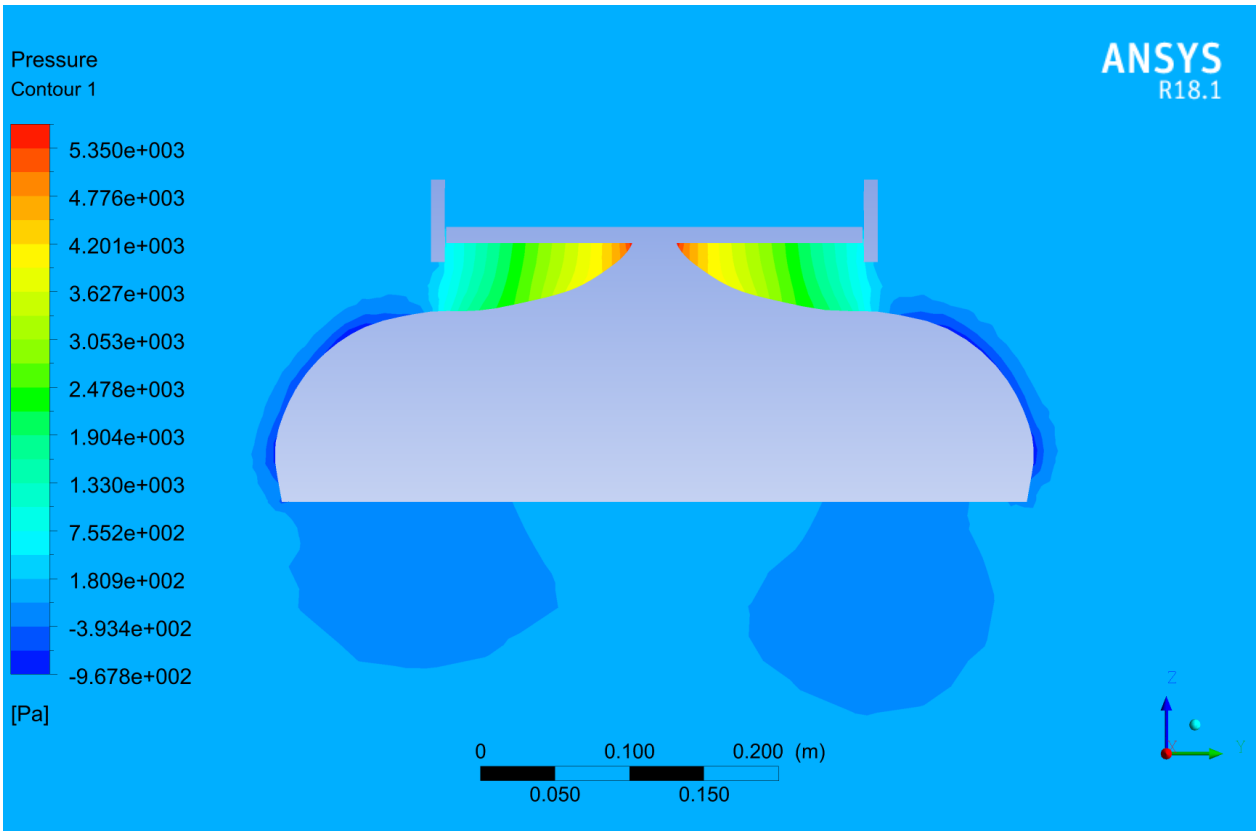

Figure 3.5 Baseline model 1 pressure contours

called as wake region has a low pressure as compared to the surroundings which contributes to the Coanda UAV drag. Altogether this type of arrangement where propeller is used is not favorable rather it decreases the lift produced by the propeller alone. This type has only a little advantage in terms of safety from exposed propeller like in quad copters and location of payload is not directly in the air stream. From fig (6), which is a Coanda UAV having centrifugal fan as a propulsion device. A centrifugal fan intakes air from above and pushes out at 90 degrees to the intake radially. As the air flow from the fan starts, flow sticks to the convex surface as a result of viscous effects and follow the curvature of the UAV. During this, there is entrainment of air from the above due to viscous effects resulting in a creation of low pressure area and hence lift force. As there is no downward air component because of centrifugal fan, there is no high pressure area on the UAV. Moreover, it has a uniform low pressure area above the curved surface which contributes to the

net positive lift of the Coanda UAV. In spite of the positive lift it also has a low pressure wake region contributing to the drag.

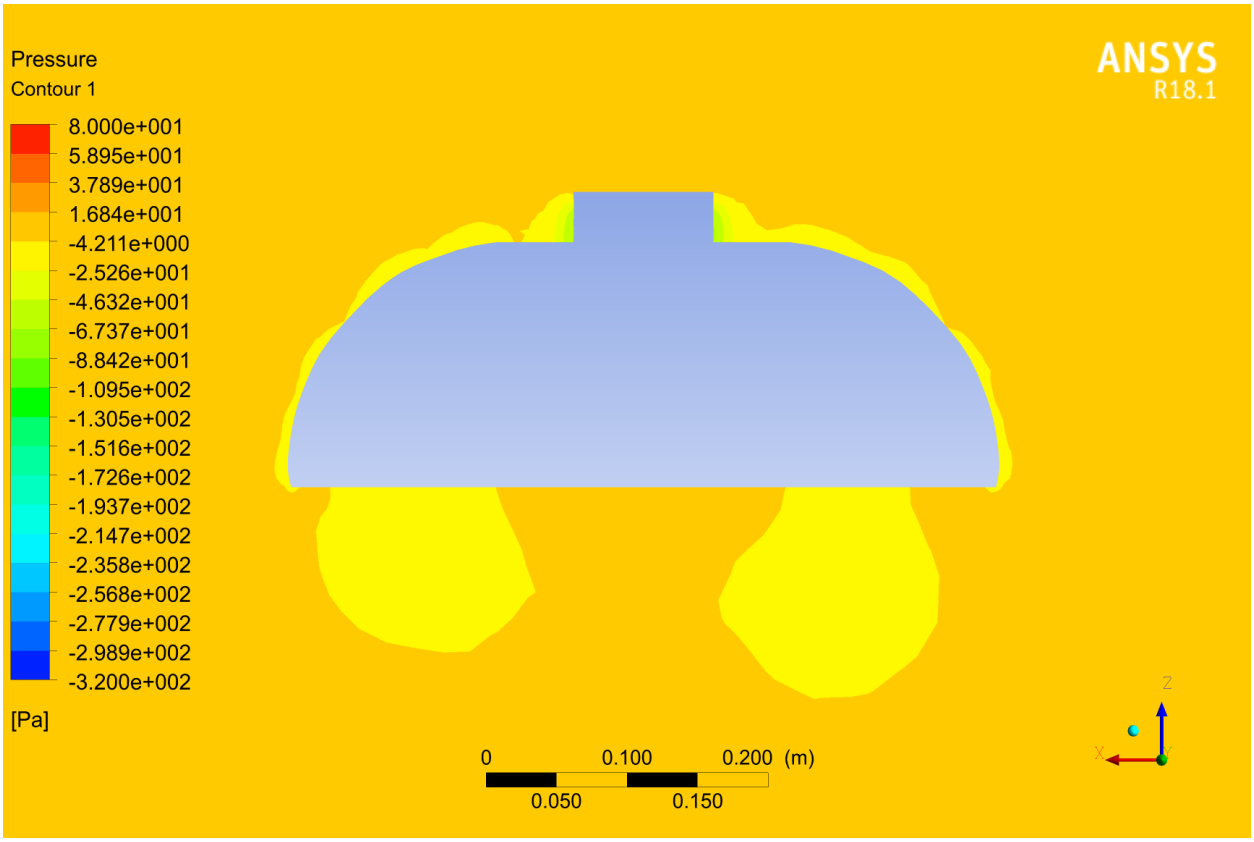

Figure 3.6 Baseline model 2 pressure contours

CHAPTER 4: RESULTS AND DISCUSSION

4.1 Design Variation

After analyzing the pressure variation of two baseline models, in order to increase the aerodynamic efficiency of Coanda UAV, two pertinent areas should be addressed. Firstly, design of curved surface responsible for lift generation should be optimized to generate maximum lift and secondly wake region underneath the Coanda UAV should be reduced to decrease drag. These two measure will enhance the lift of a Coanda UAV which can be translated into more endurance and range. In view of this, we have investigated two cases which are double convex surface and extensions / skirt to the lower part to reduce wake.

4.1.1 Double convex surface

A novel design which consists of double convex surface instead of one is modelled. There are few authors who studied and experimented with different shapes of a single convex surface in which Bernstein polynomial and other optimization techniques were used to optimize the convex surface but there is no such study on double convex surface. In this case, a double convex surface Coanda UAV having the same dimensions of baseline models. Numerical analysis was performed using same boundary conditions. Results show an increase of 5.52 % in lift. Pressure contours in fig (9) depict a lower surface pressure on the curved surface as compared to the baseline model which is evident from increase in lift. In addition to this, pressure below the UAV is slightly less negative in the wake region.

4.1.2 Extension of lower side /skirt

As previous case shows positive results, we have setup another case which aims at reducing the wake. Commonly, in aerodynamics to reduce the wake which contributes to pressure drag, body is streamlined similarly to a tear drop shape. We have extended the lower side by a 15 mm in length making an angle of 45 degrees with the horizontal axis to direct the flow towards the center below the body to mix high pressure flow with the low pressure vortices and hence increase in the overall pressure below the body which pushes the UAV upwards. Again, similar boundary

conditions were employed to carry out analysis. Fig (10) shows pressure contours of second case and extension / is highlighted by black lines. As seen from the figure, major portion under the body now has positive pressure which is favorable for lift increment. Results show an increase of 9.4 % in lift as compared to the lift in double convex shape and an increase of 15.6 % compared to the baseline model. After these two modifications which have positive outcome, there is need to further explore the design space to optimize these two features to extract the maximum lift possible from this UAV. In this regard optimization algorithm is used which will be explained in the next section.

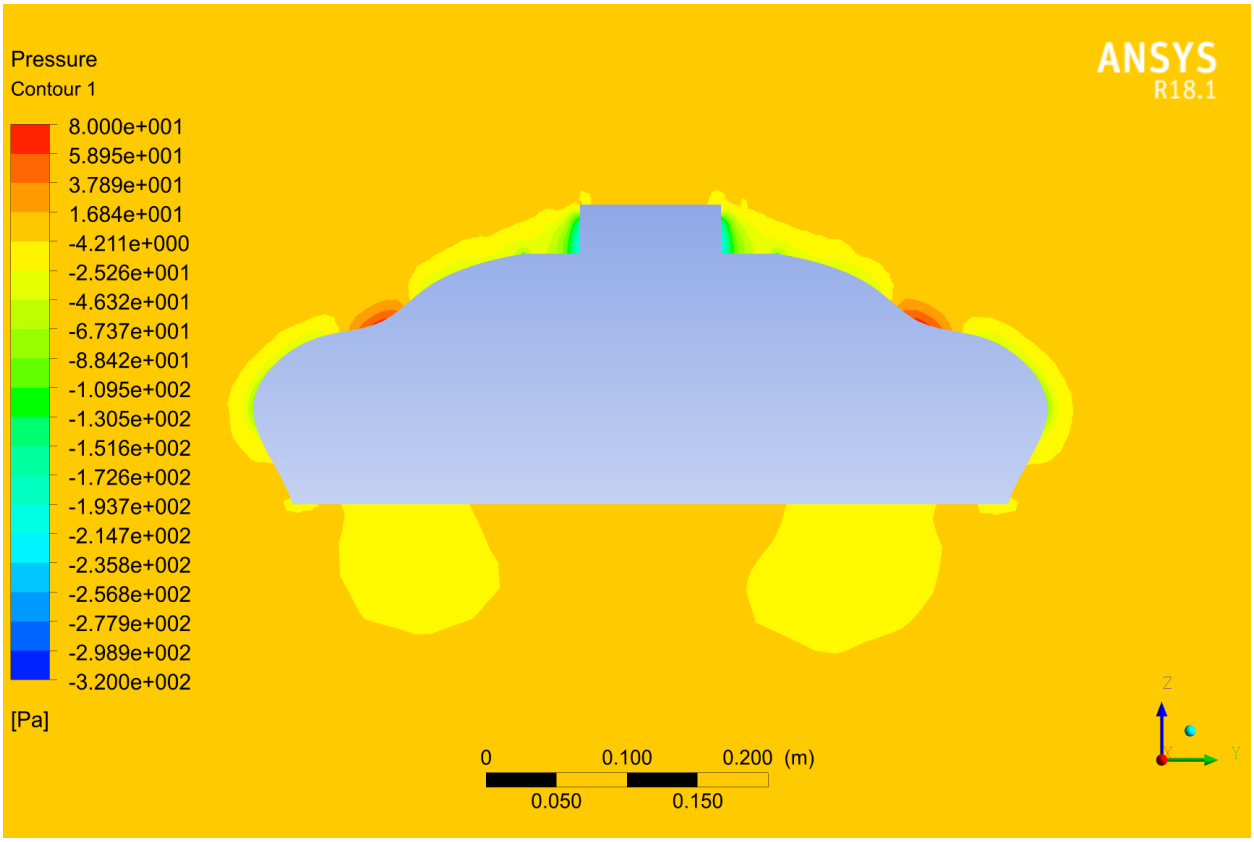

Figure 4.1 Double convex surface pressure contours

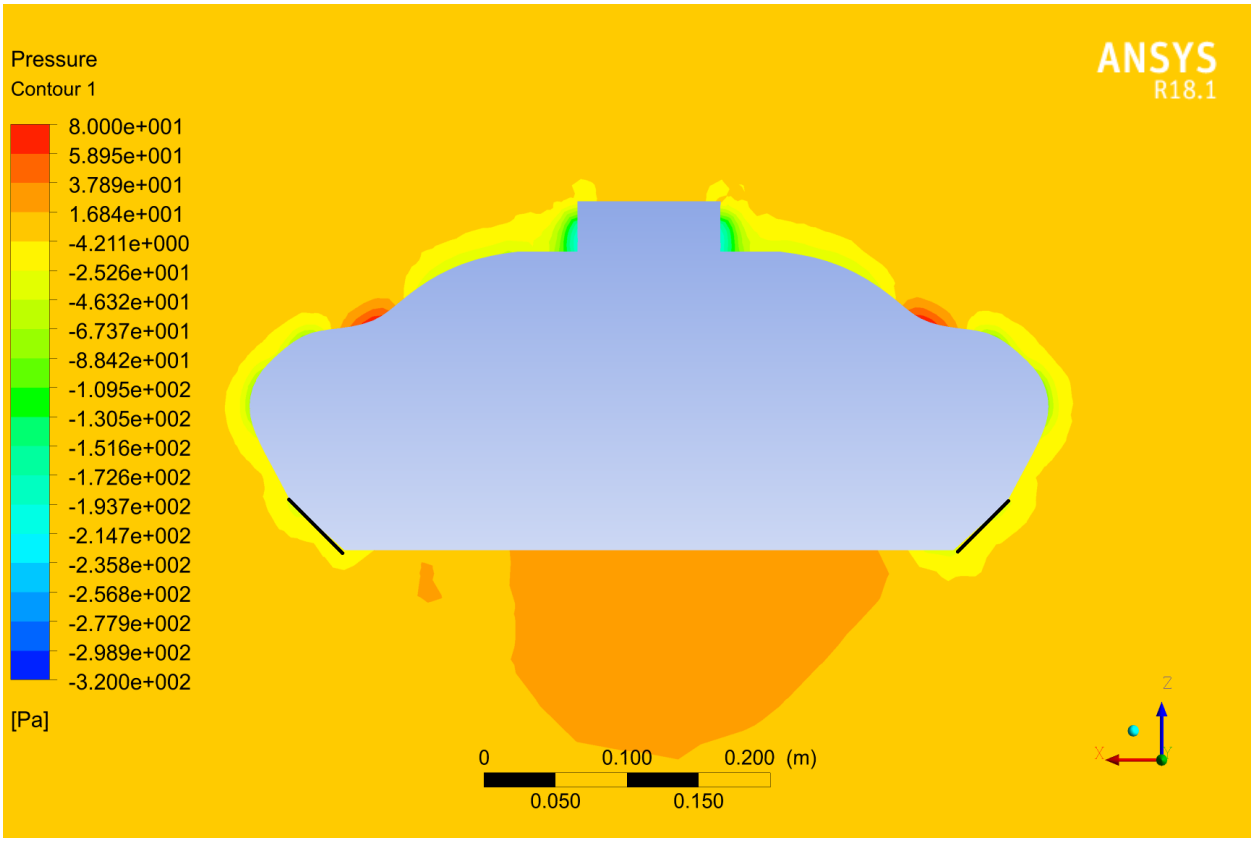

Figure 4.2 Double convex surface with skirts pressure contours

4.2 Design Optimization

Optimization has become essential in all disciplines. Simulating a given problem and iteratively exploring the designs has been very worthful, but it is also evident that the number of possible design variations are too large for reliable evaluation, so an automated assistance is needed to find the optimum solution. The ultimate aim of any computational simulation method is to automatically find the global optimum shape instead of just analysis of the given shape. Classical aerodynamics theorist have recognized the importance of optimal aerodynamic design. Let the objective function which is to be maximize or minimize with respect to the design variables β and Incompressible Navier-Stokes equations represented by R. The problem of optimization in this case becomes

Maximize $O(v, w, \beta)$ with respect to β (4.1)

Subject to **R** $(v, w, \beta) = 0$ in Ω,

where (v, w) denote flow variables in the fluid domain Ω. Lagrange function 'L' is used to merge objective function with constraints of equality constraints represented by the following equation

$$L = I + \int_{\Omega} \Psi^T . R \, d\Omega \quad (4.2)$$

In this Lagrangian equation Ψ denotes the adjoint variables. Adjoint solver process flow chart is depicted in fig (12). At first the gradients are calculated by differentiating a desired quantity with respect to the input variables. Then the sensitivities of different variables are recorded and vectors are drawn which show the direction of movement of geometry for improved performance. Sensitivity of the observed value with respect to grid node locations is

$$\delta\,(lift) = \sum_{mesh} W^n \;.\; \delta x^n \quad (4.3)$$

Where **w** is the shape sensitivity coefficient and **x** denotes node displacement and **n** represent nodes. Mesh morphing tool is used to morph the control volume mesh according to the sensitivities calculated. This morphing continues until the desired optimization is achieved. This morphed mesh can export .stl file which can be used to run the flow solver from the start and results can be computed to validate the value of optimized shape. After the optimization, new shape undergoes flow simulation and results were recorded. The flow solver from the start and results can be computed to validate the value of optimized shape. After the optimization, new shape undergoes flow simulation and results were recorded. This optimization process continues for 20 iterations and after that no appreciable change was recorded in the lift. Optimization is carried out in the following sequence

- Adjoint solver is used to calculate derivative of an engineering quantity (drag, lift etc) with respect to all the inputs. Like derivative of lift with respect to shape of the object.
- Objective function is defined either to minimize or maximize a given quantity with respect to inputs.
- To maximize the lift of an airfoil, we define solution controls, convergence criteria and iterate to convergence.

- Post processing the adjoint solution, we get shape sensitivity.
- Sensitivity tells us about the change in observed value with respect to grid node location.
- Shape sensitivity is visualized by vectors which show direction in which maximum or minimum change occurs.
- Mesh morphing is used to deform the mesh according to sensitivity.
- New optimized shape has been generated and this iterative action continues until no appreciable change is noted.

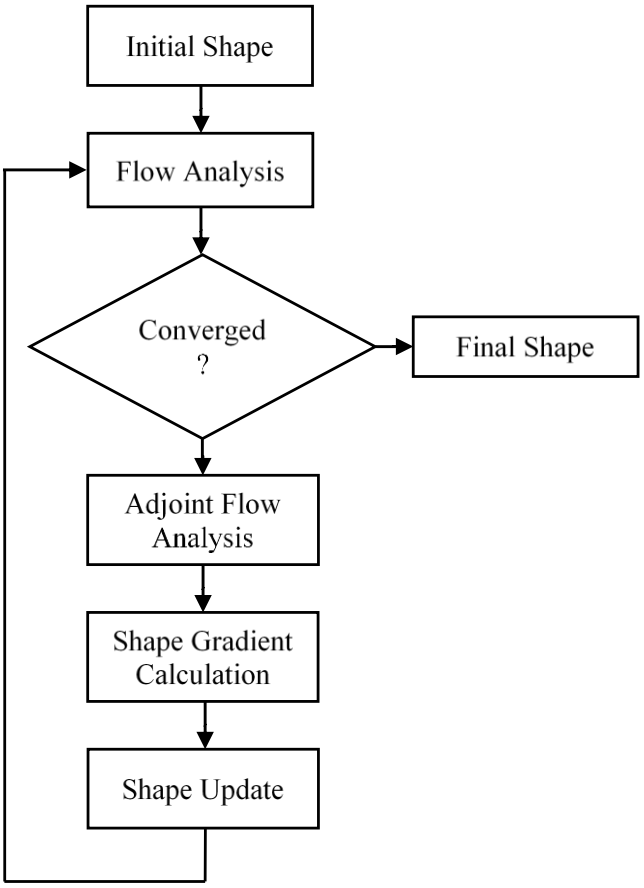

Figure 4.3 Adjoint optimization process

4.3 Results

Results are summarized in the fig (4.4), where a graph of lift versus flow velocity is depicting the lift generated by the different models having different shapes. From the graph we see that at low velocities difference is small because of less negative pressure under the UAV and the difference in Coanda blanket and velocity profile is small. As we increase the velocity there is an appreciable change in lift generated by each model. Because of the negative value of force generated by baseline model 1, it is not included in the comparison. There is an increase of 5.5 % by using double convex surface with centrifugal fan as compared a single convex surface. In addition to this, a further 9.4 % increase in lift was calculated by adding the skirt / extension to the lower side of UAV which resulted in increasing pressure on the lower side which pushes the UAV upwards and hence increase in the net force in the vertical direction called Coanda lift.

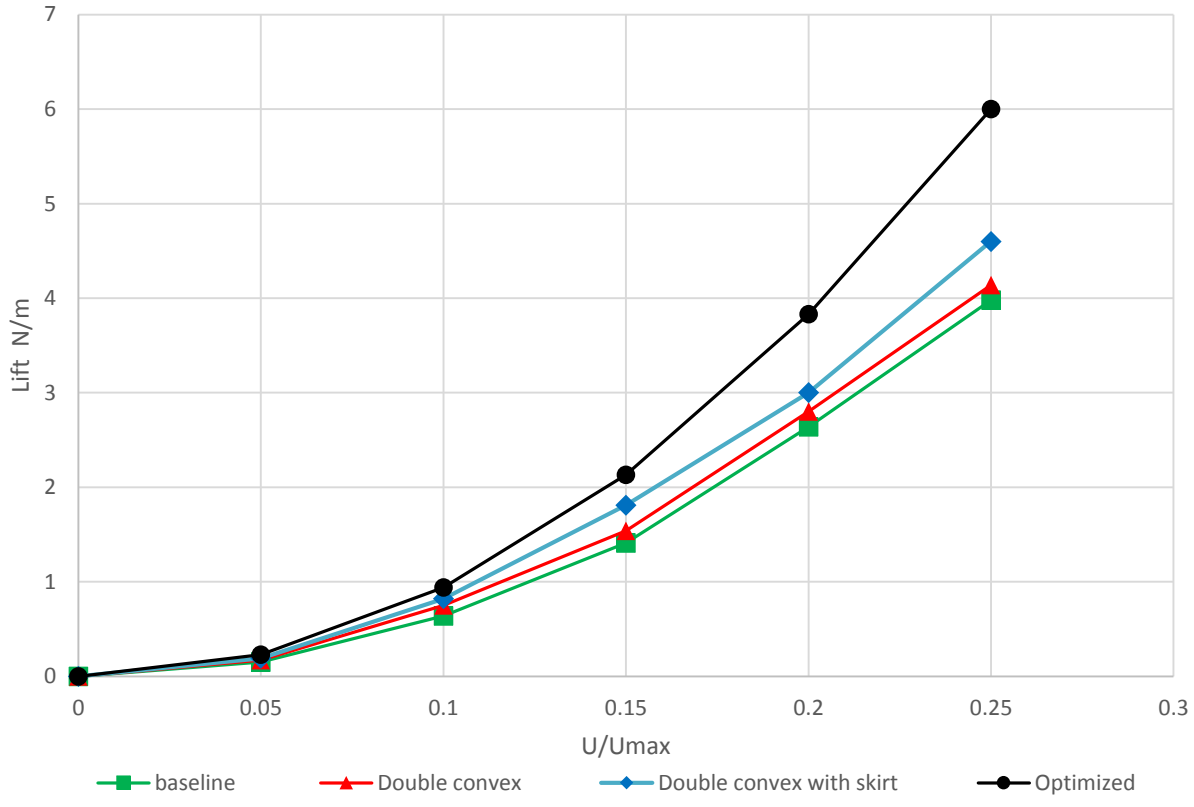

Figure 4.4 Lift vs velocity of different models

Similarly, velocity contours and streamlines show a mixing of flow from both sides and energizing the low pressure area as well as decreasing the size of the wake and pressure drag. The whole process of transformation from baseline models to the final optimized model is shown in the fig 4.5. It shows how a baseline model is improved at first using a double convex surface which works by accelerating the flow then there is a second convex surface having larger diameter to accelerate the flow further without separation of flow. And then finally skirts are used to increase the pressure underneath the vehicle for positive lift.

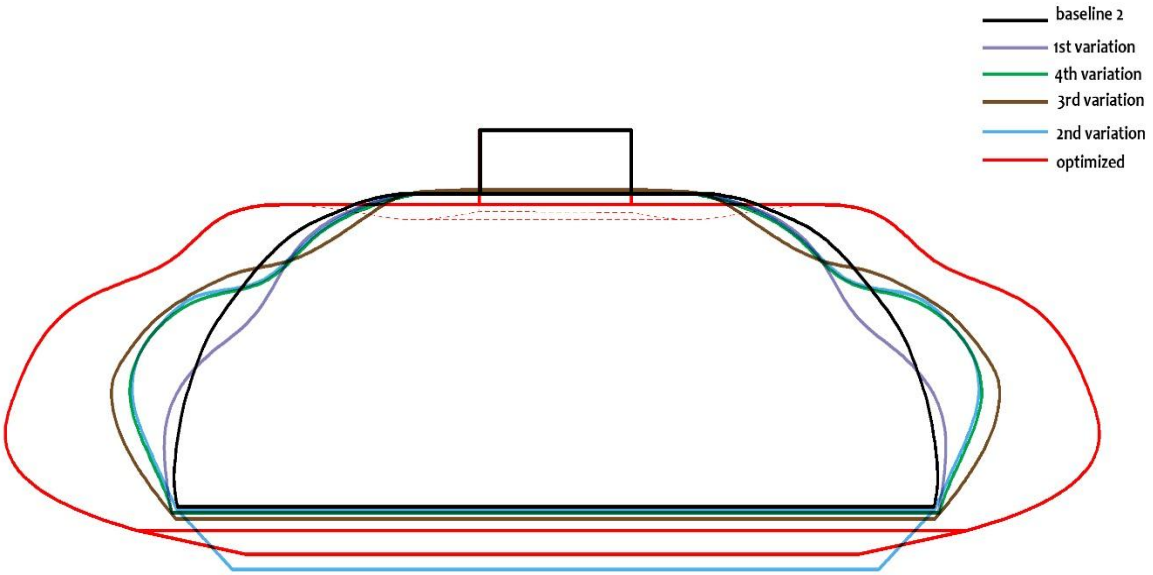

Figure 4.5 Outline of the models undergoing transformation

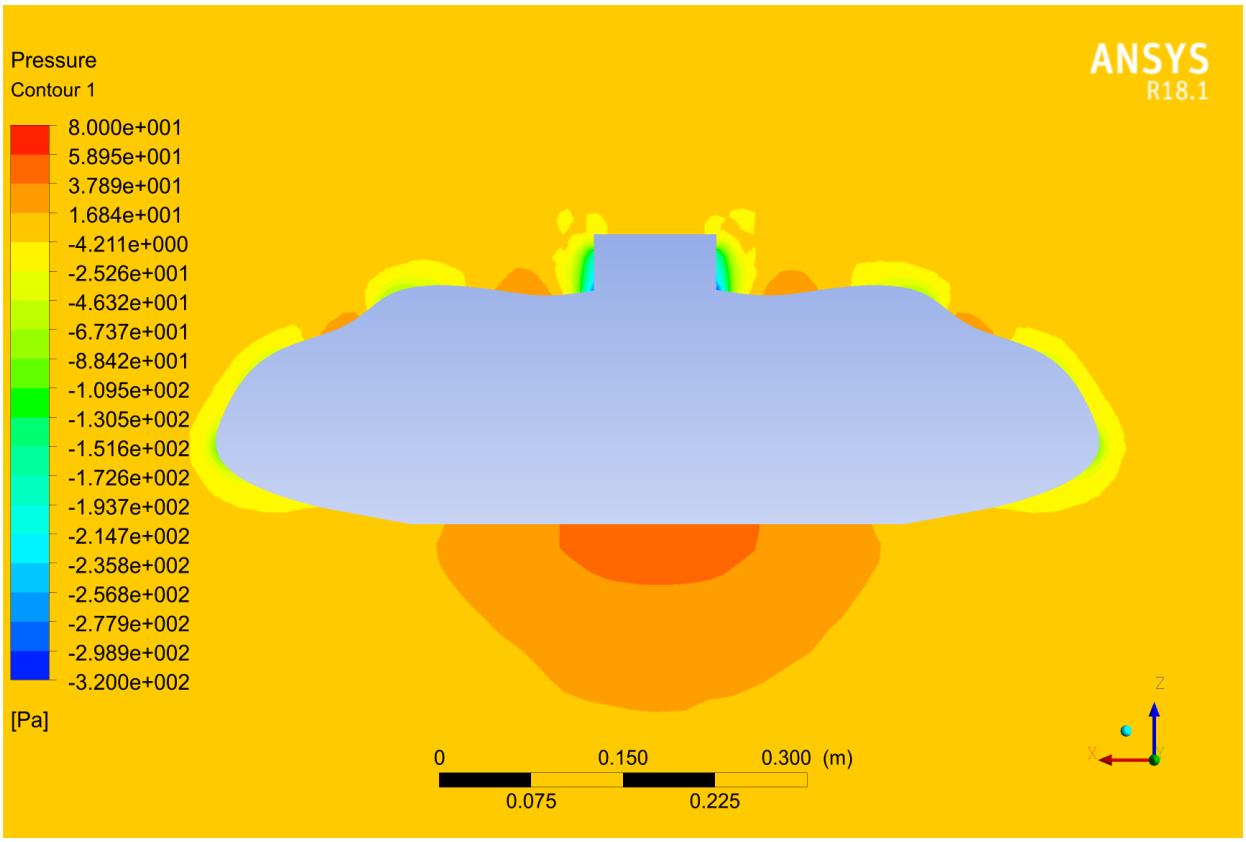

Figure 4.6 Optimized model contours of the pressure

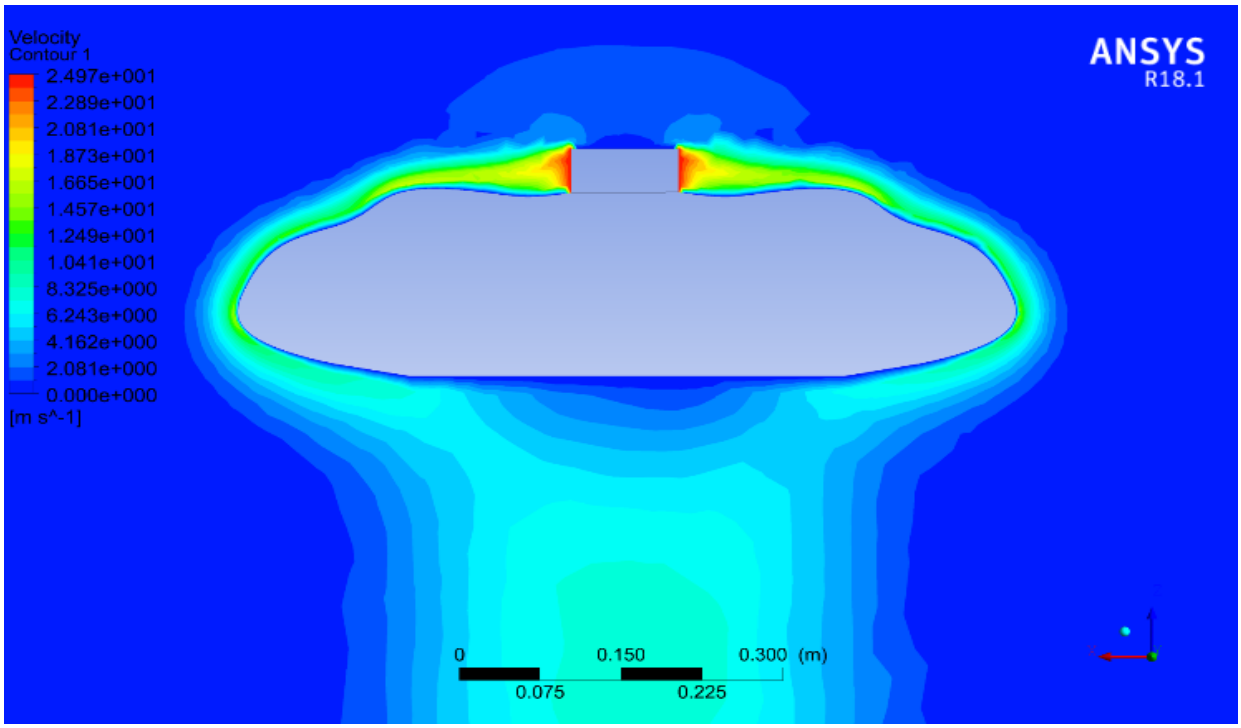

Figure 4.7 Optimized model contours of velocity

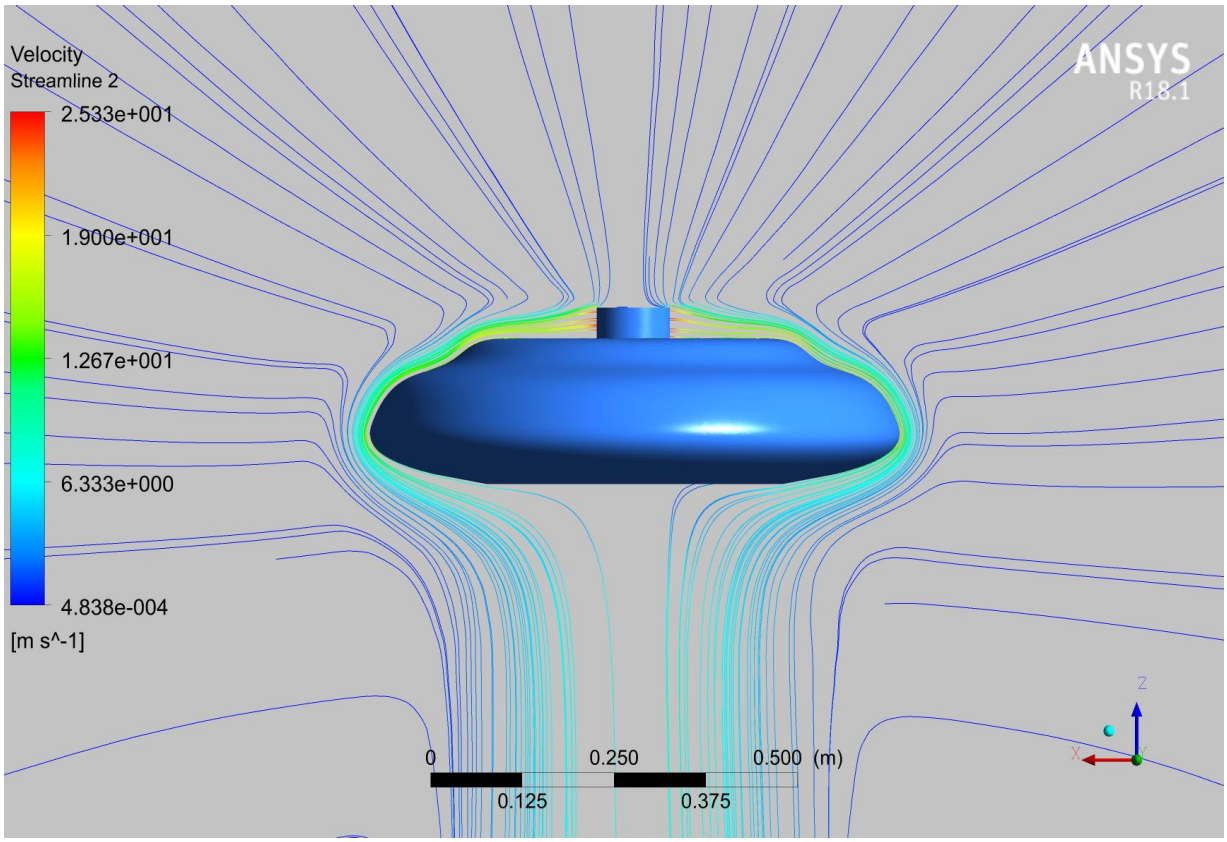

Figure 4.8 Streamlines of the optimized model

4.3.1 Angled flow

In the simulations we assume the flow is normal to the fan surface however in actual conditions flow from centrifugal fan is slightly at an angle to the fan. A simulation in which flow is at a certain angle (45) is done to check the variation in lift. Simulation shows negligible change in the lift when the flow is normal as compared to the angled flow. The streamlines showing the angled flow is shown in the fig 4.9.

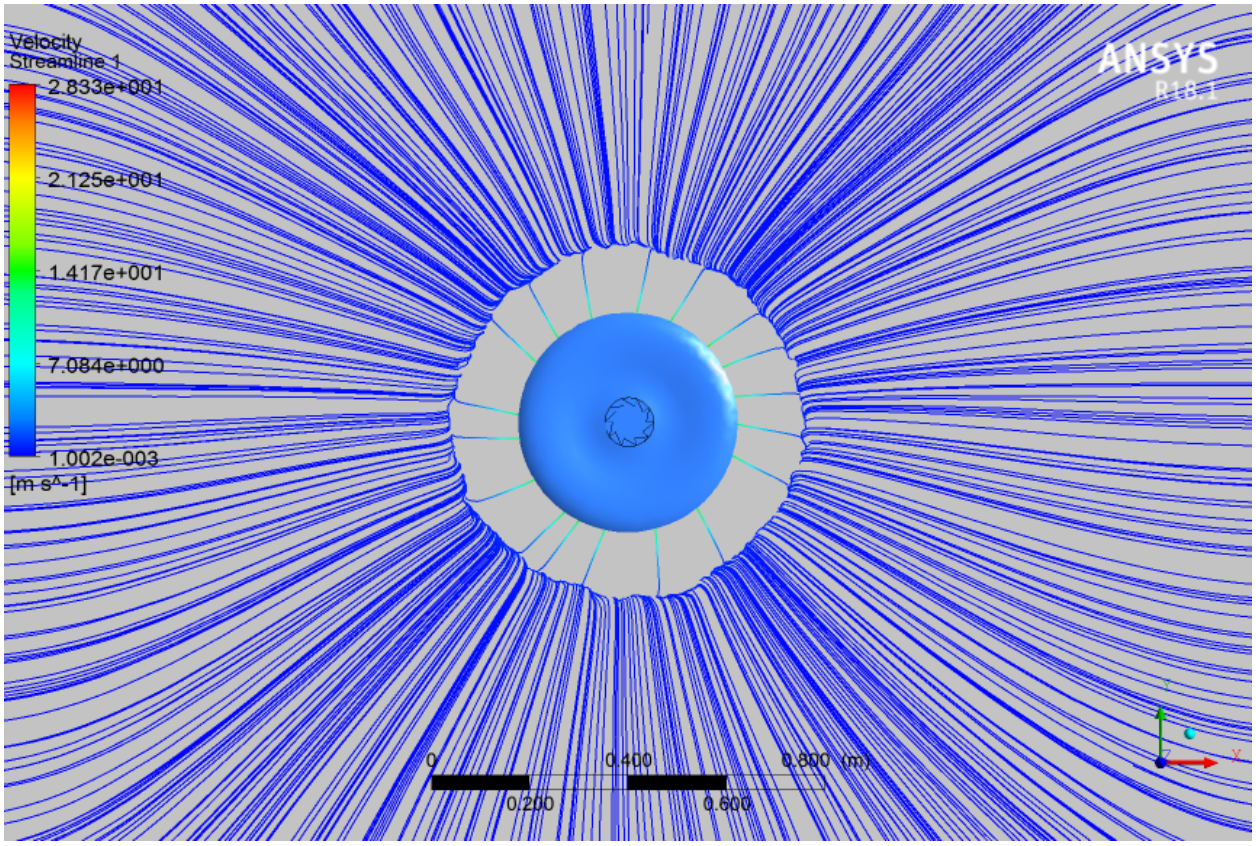

Figure 4.9 Streamlines when the flow is angled at 45 degrees

CHAPTER 5: CONCLUSION

5.1 Conclusion

In this research, we optimize the Coanda UAV lift generation capacity using CFD simulations. Two major areas were targeted namely curved surface and wake drag. Two different and most commonly used configurations in the literature were analyzed. Propeller based configuration is not favorable for Coanda UAV because the net force in the vertical direction is always negative due to high pressure downwash from the propeller. To utilize Coanda effect for lift augmentation, centrifugal fan with curved Coanda surface is the only viable choice. Moreover, centrifugal fan configuration was able to produce net positive lift but experiences penalty in terms of large wake underneath the UAV. With the introduction of novel double convex surface and skirts to the Coanda UAV and eventually optimizing it using adjoint solver, we were able to increase the lift generation capability of Coanda UAV by approximately 50 %.

5.2 Future Work

As a future work, prototyping of this novel Coanda will be carried out along with the development of flight dynamics and control system for autonomous navigation.

REFERENCES

[1] S. Hayat, E. Yanmaz, and R. Muzaffar, "Survey on Unmanned Aerial Vehicle Networks for Civil Applications: A Communications Viewpoint," IEEE Communications Surveys & Tutorials, vol. 18, no. 4, pp.2624–2661, 2016.

[2] Coanda, H. "US Patent# 2,052,869." Device for Deflecting a Stream of Elastic Fluid Projected into an Elastic Fluid (1936).

[3] Coanda H. (1936a), US Patent n. 3,261,162, Lifting Device Coanda Effect, USA.

[4] J. L. Naudin, (2006, March 10). The GFS UAV project [Online]. JLN Labs. http://jlnlabs.online.fr/gfsuav/index.htm [2010, April 21].

[5] J. T. K. Ping et al., "Preliminary design of vertical take-off and landing (VTOL) UAV with steerable vertical thrust effect," 2010 IEEE Conference on Robotics, Automation and Mechatronics, Singapore, 2010, pp. 275-279.

[6] J. T. K. Ping et al., "Coanda effect test bench (CoETB): Design enhancement of the Coanda JLT craft," in Proc. IEEE Conf. Sustain. Utilization Develop. Eng. Technol., Semenyih, Malaysia, 2011, pp. 25–30.

[7] J. Jeon et al., "Design and control of an unmanned aerial vehicle (UAV) based on the Coanda effect," in Proc. 10th Int. Conf. Ubiquitous Robots Ambient Intelligence., 2013, pp. 129–129.

[8] Barlow, Chris & Lewis, Darren & Prior, Stephen & Odedra, Sid & Erbil, Mehmet & Karamanoglu, Mehmet & Collins, Bob. (2009). Investigating the use of the Coanda Effect to create novel unmanned aerial vehicles.

[9] S. Han et al., "A flying saucer lifted with Coandă effect," 2014 IEEE International Conference on Robotics and Automation (ICRA), Hong Kong, 2014, pp. 2561-2561.

[10] H. Lee *et al*., "Design Optimization, Modeling, and Control of Unmanned Aerial Vehicle Lifted By Coandă Effect," in *IEEE/ASME Transactions on Mechatronics*, vol. 22, no. 3, pp. 1327-1336, June 2017.

[11] H. Djojodihardjo, R. I. Ahmed and A. Yousefian, "An analysis on the lift generation for Coandă micro air vehicles," 2014 IEEE International Conference on Aerospace Electronics and Remote Sensing Technology, Yogyakarta, 2014, pp. 164-169.

[12] H. Djojodihardjo, M. F. Abdul Hamid, A. A. Jaafar, et al., "Computational Study on the Aerodynamic Performance of Wind Turbine Airfoil Fitted with Coandă Jet," Journal of Renewable Energy, vol. 2013, Article ID 839319, 17 pages, 2013.

[13] Harijono Djojodihardjo (September 6th 2017). Overview of Coandă MAV as an Aerial Robotic Platform, Aerial Robots - Aerodynamics, Control and Applications, Omar Dario Lopez Mejia and Jaime Alberto Escobar Gomez, IntechOpen, DOI: 10.5772/intechopen.70157.

[14] Mirkov N, Rasuo B. Maneuverability, of a UAV with Coandă Effect Based Lift Production. International Congress of the Aeronautical Sciences; 2012. pp. 1-6.

[15] Gan, CaiYin & Sahari, Ksm & Tan, ChingSeong. (2015). Numerical investigation on Coanda flow over a logarithmic surface. Journal of Mechanical Science and Technology. 29. 2863-2869. 10.1007/s12206-015-0615-y.

[16] J. Y. Lee, S. H. Song, H. W. Shon, H. R. Choi and W. Yim, "Modeling and control of a saucer type Coandä effect UAV," *2017 IEEE International Conference on Robotics and Automation (ICRA)*, Singapore, 2017, pp. 2717-2722.

[17] Banazadeh, Afshin & Behroo, Mahan. (2015). Development, instrumentation, and dynamics identification of a Coanda air vehicle. IEEE Aerospace and Electronic Systems Magazine. 30. 4-12. 10.1109/MAES.2015.140165.

[18] Schramm, Matthias & Stoevesandt, Bernhard & Peinke, Joachim. (2018). Optimization of Airfoils Using the Adjoint Approach and the Influence of Adjoint Turbulent Viscosity. Computation. 6. 5. 10.3390/computation6010005.

[19] F. R. Menter. "Two-equation eddy-viscosity turbulence models for engineering applications", AIAA Journal, Vol. 32, No. 8 (1994), pp. 1598-1605.

[20] Tzanakis, A.B. (2014). Duct optimization using CFD software `ANSYS Fluent Adjoint Solver'.

[21] Forster, Matt & Biava, Massimo & Steijl, Rene. (2015). Optimisation of Coanda Surfaces for Transonic Circulation Control. 10.13140/RG.2.1.3675.8242.

[22] B. Wessapakdee *et al.*, "An experimental and computational fluid dynamic study of axis-symmetric Coanda configuration for VTOL MAV applications," *Appl. Mech. Mater.*, vol. 629, pp. 42–47, Oct. 2014.

[23] J. Kweder, C. C. Panther and J. E. Smith, Applications of circulation control, yesterday and today, *International Journal of Engineering*, 14 (5) (2010) 411-429.

[24] B. Saeed and G. B. Gratton, An approach to evaluate lift generated by an annular-Coanda-wing for vertical/short takeoff and landing applications, *Proceedings of the Institution of Mechanical Engineers, Part G: Journal of Aerospace Engineering*, 226 (10) (2012) 1298-1314.

[25] Dumas, A., Subhash, M., Trancossi, M., and Marques, J. P., The Influence of Surface Temperature on Coanda Effect, Energy Procedia Vol. 45, 2014, pp. 626-634.doi: 10.1016/j.egypro.2014.01.067, 2014.

[26] ANSYS FLUENT Manual. ANSYS FLUENT Adjoint Solver. Version 18.1. ANSYS, Inc., 2018.